

# Pathophysiological aspects of cystocele with a 3D finite elements model

Géry Lamblin<sup>1,2,3</sup> · Olivier Mayeur<sup>4,7</sup> · Géraldine Giraudet<sup>3,5,6</sup> ·  
Estelle Jean dit Gautier<sup>3,5,6</sup> · Gautier Chene<sup>1,2</sup> · Mathias Brieu<sup>4,7</sup> ·  
Chrystèle Rubod<sup>3,4,5,6</sup> · Michel Cosson<sup>3,4,5,6</sup>

Received: 14 March 2016 / Accepted: 6 July 2016 / Published online: 11 July 2016  
© Springer-Verlag Berlin Heidelberg 2016

## Abstract

**Purposes** The objective of this study is to design a 3D biomechanical model of the female pelvic system to assess pelvic organ suspension theories and understand cystocele mechanisms.

**Methods** A finite elements (FE) model was constructed to calculate the impact of suspension structure geometry on cystocele. The sample was a geometric model of a control patient's pelvic organs. The method used geometric reconstruction, implemented by the biomechanical properties of each anatomic structure. Various geometric configurations were simulated on the FE method to analyse the role of each structure and compare the two main anatomic theories.

**Results** The main outcome measure was a 3D biomechanical model of the female pelvic system. The various configurations of bladder displacement simulated mechanisms underlying medial, lateral and apical cystocele. FE simulation revealed that pubocervical fascia is the most

influential structure in the onset of median cystocele (essentially after 40 % impairment). Lateral cystocele showed a stronger influence of arcus tendineus fasciae pelvis (ATFP) on vaginal wall displacement under short ATFP lengthening. In apical cystocele, the uterosacral ligament showed greater influence than the cardinal ligament. Suspension system elongation increased displacement by 25 % in each type of cystocele.

**Conclusions** A 3D digital model enabled simulations of anatomic structures underlying cystocele to better understand cystocele pathophysiology. The model could be used to predict cystocele surgery results and personalising technique by preoperative simulation.

**Keywords** Cystocele · Functional anatomy · Pelvic displacement · Finite elements simulation · Computational modelling

## Abbreviations and acronyms

ATFP Arcus tendineus fasciae pelvis  
ATLA Arcus tendineus levator ani  
FE Finite elements

## Introduction

The phenomena underlying female genital prolapse are multifactorial: parity, history of vaginal delivery, age, obesity, and also biomechanical deficiency in the ligamentous, fascial and muscular support structures [1–5]. Cystocele is the commonest form and is pathophysiologically complex [6, 7]. The anatomic defects involved remain unclear, despite the advent of biomechanical models [6, 8, 9]. The respective roles of each component of anterior pelvic support are controversial, with several anatomic

✉ Géry Lamblin  
gerly.lamblin@chu-lyon.fr

<sup>1</sup> Department of Urogynecology, HFME, HCL, Femme Mère Enfant University Hospital, 59 Boulevard Pinel, Lyon-Bron, 69677 Bron, France

<sup>2</sup> University of Claude Bernard Lyon 1, Villeurbanne, France

<sup>3</sup> University of Medicine Henri Warembourg, Lille University, Villeneuve-d'Ascq, France

<sup>4</sup> FRE 3723-LML-Laboratoire de Mécanique de Lille, Univ. Lille, 59000 Lille, France

<sup>5</sup> Department of Urogynecology, Jeanne de Flandre Hospital, Lille, France

<sup>6</sup> Lille 2 University, Lille, France

<sup>7</sup> Centrale Lille, Cité Scientifique CS 20048, 59000 Lille, France

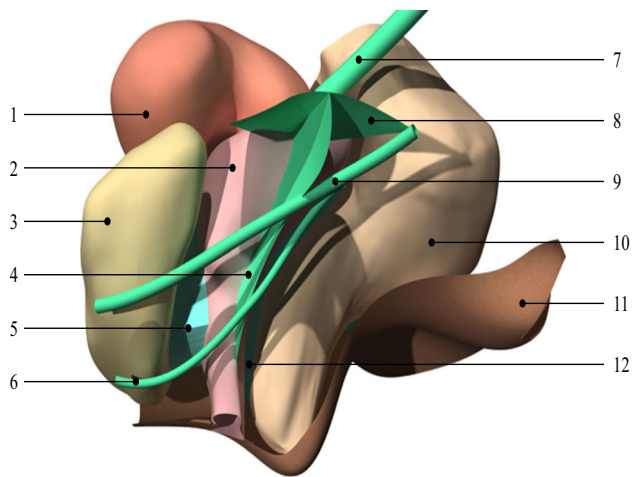


**Fig. 1** 3D digital model of the pelvic floor. (1) Uterus. (2) Vagina. (3) Bladder. (4) Endopelvic fascia. (5) Pubocervical fascia. (6) ATFP. (7) Uterosacral ligament. (8) Cardinal ligament. (9) ATLA. (10) Rectum. (11) Pelvic floor. (12) Rectovaginal fascia

theories [10–14]. Petros and DeLancey developed two of the most complete theories of pelvic floor [10–13]. DeLancey’s theory, based on anatomic models and MRI, provides a 3-level anatomopathological definition of prolapse. Petros’s “integral” theory describes the interdependence of organs via their support systems, with a direct relation between ligament-fascia lesions and clinical expression [10, 11]. Both aim to assess a relationship between anatomical impairment and symptoms, but attribute different roles to the implicated ligament structures.

This study assessed bladder suspension structures separately according to these two main anatomic theories and the structures which are considered essential to cystocele onset: pubocervical fascia, endopelvic fascia, arcus tendineus fasciae pelvis (ATFP), arcus tendineus levator ani (ATLA), uterosacral ligament, and cardinal ligament [10–13] (Fig. 1).

The study objective was to design a 3D biomechanical model of the female pelvic system, incorporating these essential components of bladder suspension, and simulate the bladder displacements involved in cystocele. The impact of each ligamentous and fascial structure on onset of the three types of cystocele (medial, lateral, apical) was analysed. A finite elements (FE) model was constructed to calculate the respective geometric impacts of the anatomic structures on cystocele onset, shedding light on underlying pathophysiology.

## Methods

The study was registered with the local audit committee; written informed consent was obtained from the control subject. This control subject was a young woman aged

30 years without prolapse or other pelvic pathology on clinical examination. Pelvic MRI was performed supine, with high-resolution T1- and T2-weighted coronal, axial and sagittal sequences (slice thickness, 3 mm; interval, 3 mm, voxel size, 0.48–0.72 mm; resolution, 512 × 512). Only T2 static sequences were used to construct the FE model.

First, a 3D representation of the pelvic system was generated with manual delimitation of each structure of interest: uterus, vagina, bowel, pubocervical fascia, endopelvic fascia, ATFP, ATLA, uterosacral ligament, cardinal ligament and levator ani muscle. Each organ was delineated, segmented in terms of its outer walls, and reconstructed in 3D, using Avizo™ 7 software (Fig. 1). MRI segmentation was transformed into a 3D representation composed of unstructured triangulated surfaces, using the Avizo™ software, then converted into an organised surface model using Catia™ software, producing smoother, more representative surfaces for FE meshing (Fig. 2). The FE method is commonly used to investigate organ mobility and the mechanisms involved, and to highlight patient-specific aspects [9]. Stress was defined at the limits of the model, i.e. the expected behaviour of various organs in physiological condition, taking behaviour of each organ as isotropic [15]. Physiological conditions were reproduced by simulating a  $10^{-3}$  MPa (or 10 cm H<sub>2</sub>O in urodynamics) cough effort applied on the upper parts of bladder and uterus, with an inclined surface force 45° to the subject’s vertical axis [9, 16, 17]. Displacement was analysed at each point of the FE model and compared to baseline in each configuration. The model was supplemented with the biomechanical properties of each anatomic structure, following the literature [15, 18, 19]. Table 1 presents the elements employed in simulation, thicknesses of shell elements and number of elements per structure (Table 1).

The various structures involved in the various forms of cystocele were simulated using Abaqus/CAE 6.12-2 software. This software allows us to perform simulations of the FE method. Anatomical structures are modelled by FE meshing to reproduce accurately the structures involved (surface continuity, regularity of meshing). Several types of elements are used to model the structures, using three-dimensional (hexahedral element), two-dimensional (shell/quad elements) or one-dimensional representation (beam element) [9, 20]. Following the Abaqus library, shell elements were used for organs with constant thickness (and hexahedral elements for the uterus), shell elements for ligaments (and beam for the uterosacral ligament), and solid elements for fasciae. To validate FE mesh quality, a convergence test was conducted, rendering an adequate mesh of 40,000 elements. For boundary conditions, pelvic floor was modelled by a representative surface sustaining organs and ligamentous structures, with edges fixed near

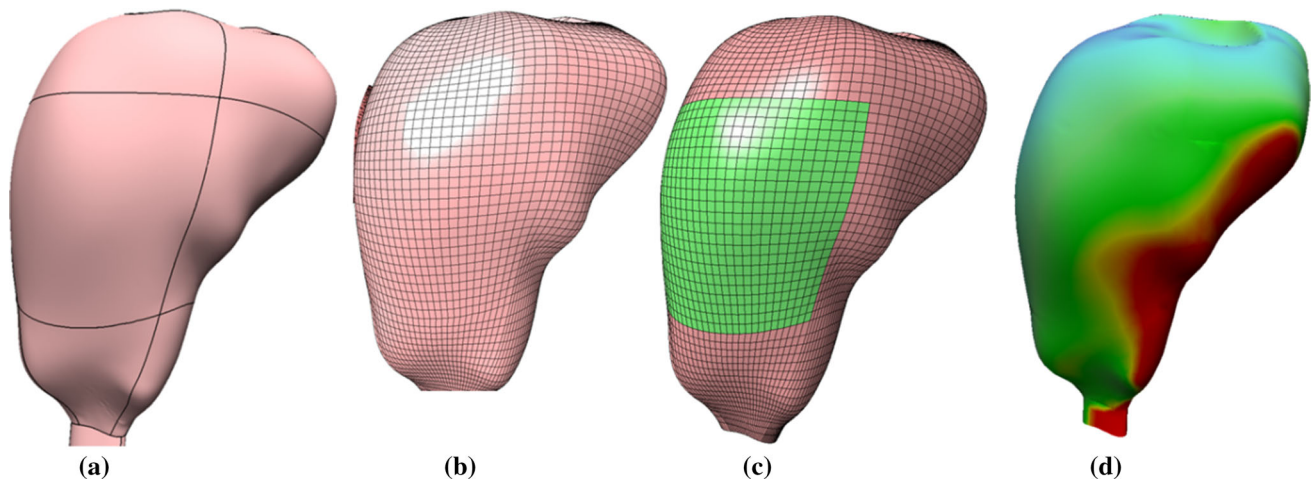


**Fig. 2** Finite elements model generation (example of vagina). **a** Surface representation (CAD). **b** Meshing. **c** In green: interface between vagina and pubocervical fascia. **d** Iso-values of displacement

**Table 1** Mechanical properties of pelvic soft tissue and FE model data (element type, thickness and number) [8, 18]

	Young's modulus (MPa)	Element Type <sup>d</sup>	Thickness (mm)	Element Nb
ATLA <sup>a</sup> and ATFP <sup>b</sup>	0.78	Quad	2	1 k
Bladder	0.24	Quad	2	3.6 k
Cardinal ligament	1.32	Quad	1	2.7 k
Endopelvic fascia	2.22	Quad	1	2.1 k
PCF <sup>c</sup>	0.03	Hexa	na	7 k
Pelvic floor	0.03	Quad	2	3.5 k
Rectum	0.54	Quad	3	3.7 k
Uterosacral ligament	0.78	Beam	na	0.03 k
Vagina rectum fascia	0.04	Hexa	na	8 k
Vagina	0.66	Quad	3	2.4 k

<sup>a</sup> Arcus tendineus levator ani

<sup>b</sup> Arcus tendineus fasciae pelvis

<sup>c</sup> Pubocervical fascia

<sup>d</sup> Several types of elements are used: three-dimensional (hexahedral element), two-dimensional (shell/quad elements) or one-dimensional representation (beam element)

the sacrum, pubis and bone structures. Connective tissue binding with organs used shared nodes. The first simulation without change to the endopelvic or pubocervical fascia, thus, represented baseline pelvic organ system displacement under effort, without change in geometric characteristics. For medial and lateral cystocele, bladder displacement was analysed as the displacement of three points located at the superior, middle and inferior parts of the bladder, in the direction from bladder to vagina. Likewise, three points were located in the upper vagina at the cervix for apical cystocele.

Organ displacement was described by the maximal displacement of these points. The percentage difference was calculated between the baseline configuration and that resulting from each geometric modification imposed on the

six relevant structures. This enabled differential displacement to be represented for each form of cystocele according to the two theories, taking account of the Young's modulus of the anatomic structures involved (Fig. 3). The levator ani muscle was modelled in a simplified form and not included in the final model, as it is not directly involved in these anatomic theories of cystocele.

In medial cystocele, the FE model took account of pubocervical and endopelvic fascia lengthening (configurations 2 and 3) (Fig. 3). For lateral cystocele, 2 configurations were implemented to analyse the effect of ATFP and ATLA lengthening (configurations 4 and 5). For apical cystocele, 2 configurations were generated according to uterosacral ligament and cardinal ligament lengthening (configurations 6 and 7) (Fig. 3).

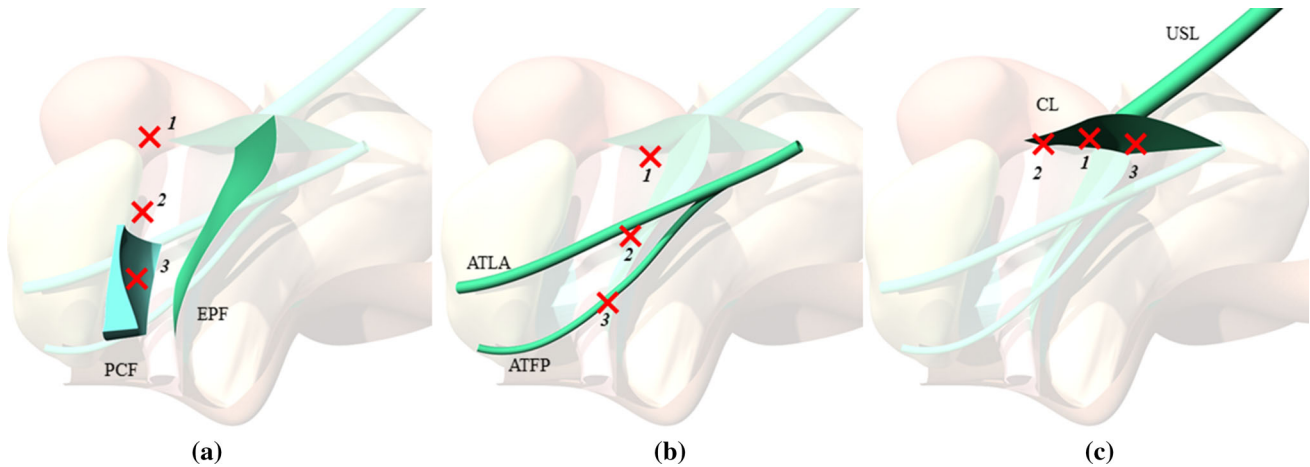


**Fig. 3** Suspension structures involved in the different configurations. *PCF* pubocervical fascia, *EPF* endopelvic fascia, *ATFP* arcus tendineus fasciae pelvis, *ATLA* arcus tendineus levator ani, *CL* cardinal ligament, *USL* uterosacral ligament, *red crosses* points located to analyse bladder displacement for each configuration. **a** For medial cystocele. *PCF* for configuration #2 and *EPF* for configuration #3. **b** For lateral cystocele. *ATLA* for configuration #4 and *ATFP* for configuration #5. **c** For apical cystocele. *USL* for configuration #6 and *CL* for configuration #7

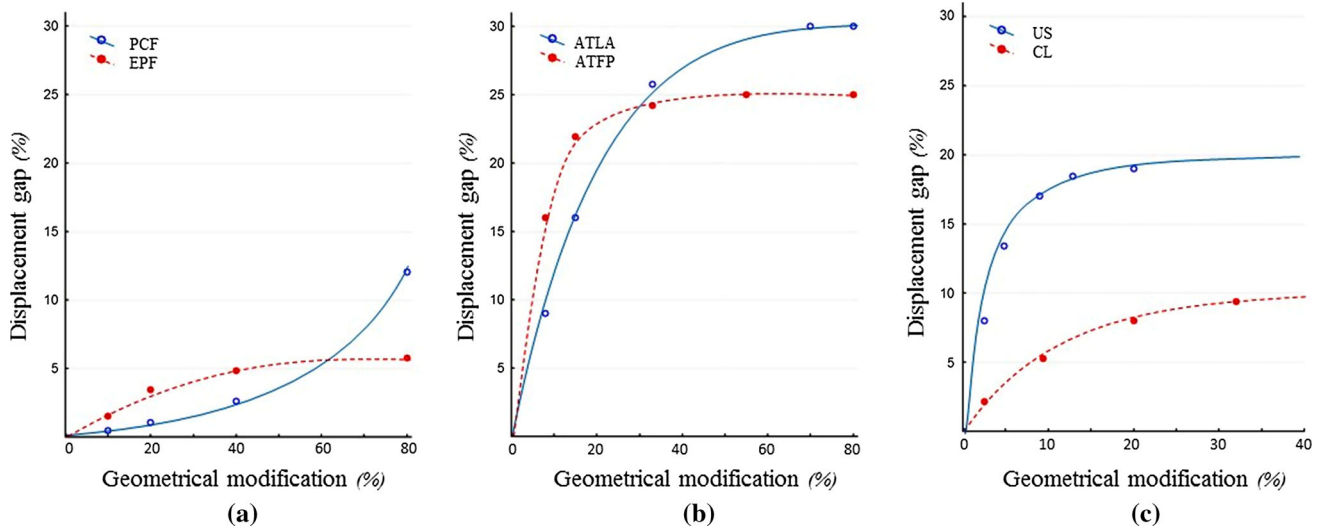


**Fig. 4** Percentage difference in displacement with: **a** pubocervical fascia (PCF) and endopelvic fascia (EPF) lengthening, **b** arcus tendineus fasciae pelvis (ATFP) and arcus tendineus levator ani (ATLA) lengthening, **c** uterosacral ligament (USL) and cardinal ligament (CL) lengthening. In medial cystocele, after 40 % pubocervical fascia lengthening, bladder displacement continued to increase

(a). In lateral cystocele, 8 % ATLA lengthening induced less than 10 % difference with respect to baseline. With 8 % ATFP lengthening, the difference was 15 % (b). In apical cystocele, as of 10 % USL lengthening, bladder displacement rapidly reached 20 % (c)

**Results**

FE simulation of the various bladder displacements between baseline and effort allowed different analyses of each structure involved in each form of cystocele (medial, lateral, apical) (Fig. 4). In medial cystocele, the two anatomic structures involved (pubocervical fascia and endopelvic fascia) made a major contribution to the pathophysiological mechanisms (Fig. 4a), pubocervical fascia playing the

leading role with increasing pubocervical fascia lengthening, bladder displacement increased linearly and significantly for each study point. After 40 % pubocervical fascia lengthening, bladder displacement continued to increase. In contrast, after 40 % endopelvic fascia lengthening the rate of increase in bladder displacement fell, with just 6 % displacement after 60 % lengthening (Fig. 4a).

In lateral cystocele, large 30 % lengthening of both ATLA and ATFP had the same effect on maximal bladder

displacement. Under shorter lengthening, impact was twice as great for ATFP as for ATLA. Under 8 % ATLA lengthening, difference from baseline was less than 10 %, while equivalent ATFP lengthening gave a 15 % difference from baseline (Fig. 4b). Thus, under short lengthenings, ATFP has a greater influence on lateral cystocele displacement.

In apical cystocele, the uterosacral ligament exerted a greater influence than the cardinal ligament. After 10 % uterosacral ligament lengthening, displacement became faster and greater, reaching 20 % with respect to baseline, compared to only 10 % for cardinal ligament lengthening, no matter how great (Fig. 4c). Cardinal ligament impact on displacement continued to increase slightly after 10 % lengthening. According to the present model, apical suspension is primarily governed by the uterosacral ligament.

## Comment

FE simulations of the pelvic floor determined the respective roles of each pelvic support structure in the three forms of cystocele. Medial cystocele showed a significant role of pubocervical fascia; in lateral cystocele, the ATFP had greater influence on vaginal wall displacement under short lengthening; in apical cystocele, the uterosacral ligament played the major role.

This study created an innovative FE model of the pelvic floor, including the anatomic structures essential to understanding cystocele. The anterior vaginal wall plays a major role in supporting the bladder [10–14, 21]. It is this part of the vaginal wall, subject to abdominal pressure that induces the discomfort associated with cystocele [22].

DeLancey's "paravaginal support" theory was initially founded on anatomic models and later on MRI, with a 3-level anatomopathological definition according to the affected anatomic structures: high or apical cystocele involving failure of the superior third of the vagina, including the uterosacral and cardinal ligament origins on the cervical ring (level 1); lateral cystocele involving failure of the *arci tendinei* (level 2); and medial cystocele involving failure of the sagittal suspension system at the upper cervical ring (pubocervical fascia and/or endopelvic fascia) [10–13]. DeLancey's theory is constantly evolving with clinical experience and the development of dynamic MRI and biomechanical models [6, 22, 23].

The bladder lies on the pubocervical fascia, essential to medial cystocele. In Petros's theory, pubocervical fascia lengthening at the cervical ring is the key feature [10, 11]. In DeLancey's theory, a major role is also played by the endopelvic fascia, a connective tissue layer covering the levator ani muscle laterally; medial cystocele is induced by

lengthening of not only pubocervical but also endopelvic fascia [12, 13].

In the present model, both structures did indeed play major roles in medial cystocele, but that of the pubocervical fascia was preponderant, as Petros suggested (Fig. 4); the greater the pubocervical fascia lengthening, the greater the bladder displacement. Thus, pubocervical fascia lengthening was the essential contributor to medial cystocele according to the present biomechanical model.

Lateral cystocele results from ligamentous and fascial failure of ATLA and ATFP in the inferior/anterior part of the pubocervical fascia, forming a transverse "hammock". Lengthening of either impairs bladder support, inducing lateral cystocele [10–13]. Richardson et al., exploring high-grade cystocele, reported ATFP avulsion from the pubocervical fascia and vaginal wall in more than 90 % of cases [24]. The present biomechanical model suggests that lateral cystocele implicates an anatomic defect between the anterior vaginal wall and the ATFP, which seems to be the essential ligamentous structure involved in lateral bladder support, as suggested by both DeLancey and Petros. DeLancey also implicated ATLA in lateral cystocele, but the present model indicated a greater effect of ATFP [12, 13].

Concerning apical cystocele, recent clinical and radiological studies highlighted the apical component of pelvic organ support, although its specific contribution remains undetermined [25, 26]. The uterosacral-cardinal ligament complex directly bears on cervical statics and vaginal dome suspension above the levator floor [27]. The uterosacral ligament inserts to the cervical ring and posterosuperior angles of the vaginal fornix at the cervical orifice, while the cardinal ligament is a collagenic environment, corresponding to less well-defined endopelvic fascia structures, the supportive role of which remains controversial [10, 11].

The posterosuperior pubocervical fascia is mainly supported by the uterosacral ligament, the principal support of the posterosuperior bladder base [10–14, 28]. For Petros, apical cystocele implicates cardinal ligament failure and complete pubocervical fascia avulsion from the cervical ring; uterosacral ligament hyperlaxity destabilises the pubourethral ligament and pubocervical fascia, inducing both cystocele and urinary incontinence [10, 11]. DeLancey implicates not only the cardinal but above all the uterosacral ligament. The present model confirmed that the uterosacral ligament plays a greater role than the cardinal ligament; the greater the uterosacral ligament lengthening, the greater the apical bladder displacement (Fig. 4). Likewise, sectioning the uterosacral ligament induces descent of the uterus, cervical ring and posterosuperior bladder base [10, 13]. Clinically, McCall's culdoplasty comprising uterosacral ligament shortening, and

fixation on the medial line, repositions the vaginal floor suspension structures [29].

Clinical data suggest a strong correlation between anterior compartment (point Ba on the POP-Q classification) and apex (point C) ( $r = 0.86$ ;  $p < 0.0005$ ), especially in high-grade cystocele [22, 26]. Dynamic MRI confirmed a strong correlation between anterior and apical prolapse ( $r = 0.73$ ) [26]. These findings are relevant to surgical treatment of cystocele accompanied by uterine prolapse or primary anterior support structure impairment. The strong correlation between high-grade cystocele and cervical ring defect demonstrated by DeLancey may explain the efficacy of apical correction in isolated level 1 defect (sacrocolpopexy) or apical associated to paravaginal repair in level 1 and 2 defect.

Specific lesions underlying each form of cystocele may be visible on MRI, allowing a novel strategy redefining indications and surgical repair techniques [30].

For instance, Yousuf et al., comparing cystocele according to POP-Q and anatomic lesions on MRI, demonstrated a correlation between high-grade cystocele and cervical ring defect: 75 % of high-grade cystoceles involved uterosacral ligament and pubocervical fascia failure at the uterine isthmus insertion [22]. The higher the cystocele grade, the larger the number of severe apical suspension lesions [22]. Summers and DeLancey estimated the role of the pubocervical fascia in apical cystocele at 40 % and that of the uterosacral-cardinal ligament complex at 60 % [26]. Chen et al.'s FE biomechanical model of cystocele mechanisms implicated degradation of the levator ani muscle and apical support in cystocele onset, in parallel to increased abdominal load [6]. The present results agree with those of DeLancey's team, implicating the pubocervical fascia, arcus tendineus and uterosacral ligament in all three forms of cystocele [12, 22, 26].

In the near future, preoperative simulation should enable the results of a surgical procedure for cystocele to be predicted and the technique to be adapted to the individual patient. Indeed, a better knowledge of the anatomic pelvic system may help the clinicians in the understanding of the pathophysiological mechanisms of cystocele. The 3D digital model enables simulations of anatomic structures underlying cystocele and could provide a specific tool to choose the correct surgical technique [8].

The strength of this study lies in the digital FE model specifying the geometric impact of each support structure in medial, lateral and apical cystocele, allowing the two main theories to be tested.

The study has certain limitations. First, it was founded on data for one healthy subject; however, this avoided large-sample clinical studies and the problem of individual differences. Second, the levator ani muscle and urogenital hiatus were not part of our model but it would be

interesting to incorporate them in future studies. Third, the subject was supine for MRI, whereas it would be useful to perform MRI with the subject standing and under abdominal pressure. Another relevant study would be to calibrate an FE model on patients actually presenting cystocele and to analyse the geometry of the structures involved.

## Conclusions

We developed a refined 3D model of the pelvic floor, enabling FE simulations, incorporating the anatomic structures essential to the understanding of cystocele.

The two main anatomic theories of apical and lateral bladder suspension, DeLancey's and the integral theory of Petros, are complementary but differ in mechanisms. The present biomechanical model enabled these theories to be assessed and simulations of the various mobilities involved in cystocele to be designed. The model determined the influence of each support structure for the three forms of cystocele: apical, lateral and medial. In medial cystocele, the model identified a significant role for the pubocervical fascia; in lateral cystocele, the ATRP had greater influence on vaginal wall displacement under short lengthening; in apical cystocele, the uterosacral ligament played the major role. This FE model of the pelvic system pelvic displacement improves understanding of the pathophysiology underlying cystocele.

## Compliance with ethical standards

**Funding** None.

**Conflict of interest** The authors declare that they have no conflict of interest.

**Ethical approval** All procedures performed in the studies involving human participants were in accordance with the ethical standards of the institutional and/or national research committee and with the 1964 Helsinki declaration and its later amendments or comparable ethical standards.

**Informed consent** Informed consent was obtained from the participant included in the study. The study assessed several simulations, all based on data obtained from a healthy control subject. Under French regulations, ethical board approval is not required in such cases; the study was, however, registered with the local audit committee, and written informed consent was obtained from the control subject.

## References

1. Dietz HP (2008) The aetiology of prolapse. *Int Urogynecol J Pelvic Floor Dysfunct.* 19(10):1323–1329
2. Mothes AR, Radosa MP, Altendorf-Hofmann A, Runnebaum IB (2016) Risk index for pelvic organ prolapse based on established individual risk factors. *Arch Gynecol Obstet* 293(3):617–624

3. Vergeldt TF, Weemhoff M, IntHout J, Kluivers KB (2015) Risk factors for pelvic organ prolapse and its recurrence: a systematic review. *Int Urogynecol J* 26(11):1559–1573
4. Norton PA (1993) Pelvic floor disorders: the role of fascia and ligaments. *Clin Obstet Gynecol* 36:926–938
5. Ferrari MM, Rossi G, Biondi ML, Viganò P, Dell’utri C, Meschia M (2012) Type I collagen and matrix metalloproteinase 1, 3 and 9 gene polymorphisms in the predisposition to pelvic organ prolapse. *Arch Gynecol Obstet* 285(6):1581–1586
6. Chen L, Ashton-Miller JA, DeLancey JOL (2009) A 3D finite element model of anterior vaginal wall support to evaluate mechanisms underlying cystocele formation. *J Biomech* 42:1371–1377
7. Hendrix SL, Clark A, Nygaard I, Aragaki A, Barnabei V, McTiernan A (2002) Pelvic organ prolapse in the Women’s Health initiative: gravity and gravidity. *Am J Obstet Gynecol* 186(6):1160–1166
8. Rubod C, Lecomte-Grobras P, Brieu M, Giraudet G, Betroumi N, Cosson M (2013) 3d simulation of pelvic system numerical simulation for a better understanding of the contribution of the uterine ligaments. *Int Urogynecol J* 24:2093–2098
9. Mayeur O, Witz JF, Lecomte P, Brieu M, Cosson M, Miller K (2016) Influence of geometry and mechanical properties on the accuracy of patient specific simulation of women pelvic floor. *Ann Biomed Eng* 44(1):202–212
10. Papa Petros P, Ulmsten U (1990) An integral theory of female urinary incontinence. Experimental and clinical considerations. *Acta Obstet Gynecol Scand* 53:7–31
11. Petros PEP, Woodman PJ (2008) The integral theory of continence. *Int Urogynecol J Pelvic Floor Dysfunct.* 19:35–40
12. DeLancey JO (1992) Anatomic aspects of vaginal eversion after hysterectomy. *Am J Obstet Gynecol* 166:1717–1724
13. DeLancey J (1994) Structural support of the urethra as it relates to stress urinary incontinence: the hammock hypothesis. *Am J Obstet Gynecol* 170(6):1713–1723
14. Lamblin G, Delorme E, Cosson M, Rubod C (2015) Cystocele and functional anatomy of the pelvic floor: review and update of the various theories. *Int Urogynecol J*. doi:10.1007/s00192-015-2832-4
15. Rubod C, Brieu M, Cosson M, Rivaux G, Clay JC, de Landsheere L (2012) Biomechanical properties of human pelvic organs. *Urology*. 79(4):968
16. Kamina P, Demondion X, Richer JP, Scepti M, Faure JP (2003) Anatomie clinique de l’appareil génital féminin. *Encycl Méd Chir*. Ed Sci Méd Elsevier SAS Paris Gynécologie 10:A10
17. Cobb WS, Burns JM, Kercher KW, Matthews BD, Norton H, Heniford BT (2005) Normal intra-abdominal pressure in healthy adults. *J Surg Res* 129:231–235
18. Chantereau P, Brieu M, Kammal M, Farthmann J, Gabriel B, Cosson M (2014) Mechanical properties of pelvic soft tissue of young women and impact of aging. *Int Urogynecol J* 25:1547–1553
19. Rivaux G, Rubod C, Dedet B, Brieu M, Gabriel B, Cosson M (2013) Comparative analysis of pelvic ligaments: a biomechanics study. *Int Urogynecol J* 24:135–139
20. Mayeur O, Lamblin G, Lecomte-Grobras P, Brieu M, Rubod C, Cosson M (2014) FE Simulation for the understanding of the median cystocele prolapse occurrence. In: Bello F, Cotin S (eds) *Biomedical simulation*. Springer, Berlin, Heidelberg, pp 220–227
21. Gilchrist AS, Gupta A, Eberhart RC, Zimmern PE (2010) Biomechanical properties of anterior vaginal wall prolapse tissue predict outcome of surgical repair. *J Uro.* 183:1069–1073
22. Yousuf A, Chen L, Larson K, Ashton-Miller JA, DeLancey JO (2014) The length of anterior vaginal wall exposed to external pressure on maximal straining MRI: relationship to urogenital hiatus diameter, and apical and bladder location. *Int Urogynecol J* 25:1349–1356
23. Hsu Y, Chen L, Summers A, Ashton-Miller JA, DeLancey JO (2008) Anterior vaginal wall length and degree of anterior compartment prolapse seen on dynamic MRI. *Int Urogynecol J Pelvic Floor Dysfunct* 19:137–142
24. Richardson AC, Lyon JB, Williams NL (1976) A new look at pelvic relaxation. *Am J Obstet Gynecol* 126:568–573
25. Rooney K, Kenton K, Mueller ER, FitzGerald MP, Brubaker L (2006) Advanced anterior vaginal wall prolapse is highly correlated with apical prolapse. *Am J Obstet Gynecol* 195(6):1837–1840
26. Summers A, Winkel LA, Hussain HK, DeLancey JO (2006) The relationship between anterior and apical compartment support. *Am J Obstet Gynecol* 194:1438–1443
27. Chen L, Ashton-Miller JA, Hsu Y, DeLancey JO (2006) Interaction among apical support, levator ani impairment, and anterior vaginal wall prolapse. *Obstet Gynecol* 108(2):324–332
28. Ramanah R, Berger MB, Chen L, Riethmuller D, Delancey JO (2012) See it in 3D!: researchers examined structural links between the cardinal and uterosacral ligaments. *Am J Obstet Gynecol* 207(5):437
29. Chene G, Tardieu AS, Savary D, Krief M, Boda C, Anton-Bousquet MC, Mansoor A (2008) Anatomical and functional results of McCall culdoplasty in the prevention of enteroceles and vaginal vault prolapse after vaginal hysterectomy. *Int Urogynecol J* 19(7):1007–1011
30. Gupta S, Sharma JB, Hari S, Kumar S, Roy KK, Singh N (2012) Study of dynamic magnetic resonance imaging in diagnosis of pelvic organ prolapse. *Arch Gynecol Obstet* 286(4):953–958